

Sensorless Control of a Linearized and Decoupled Induction Motor Drive

K. Barada Mohanty, Nisit K. De and Aurobinda Routray

Abstract-- This paper presents an input-output linearizing and decoupling control scheme with speed estimation for an adjustable speed induction motor drive. A stator flux based estimator is used to estimate the synchronous speed. The motor speed is estimated by measuring only two line currents and two line voltages. A moving average algorithm is used to filter the ripples in the estimated speed. Simulation studies show that the sensorless speed control scheme can achieve fast transient response and maintain a wide speed control range.

Index Terms—Decoupling control, input-Output linearization, moving average algorithm, speed estimation.

I. INTRODUCTION

Induction motor (IM) is very widely used in industry, because of its simple and robust structure, higher torque-to-weight ratio, higher reliability and ability to operate in hazardous environment. But control of induction motor is a challenging task, as its dynamical system is nonlinear, the rotor variables are not measurable, and physical parameters are most often not accurately known. The control of the induction motor has attracted much attention in the last decade. One of the most significant developments in this area has been the linearizing control [1-4]. In [1], the IM drive is controlled for good dynamic performance and maximum power efficiency by means of linear decoupling of rotor flux and speed. Principle of nonlinear control is applied in [2] to linearize the IM drive. Decoupling of speed and flux, is achieved by static state feedback controller. In [3], decoupling of torque and flux, using the amplitude and frequency of the supply voltage as inputs, is also obtained by a static state feedback controller. Marino et. al [4] have designed a nonlinear adaptive state feedback input-output linearizing and decoupling controller for the IM drive.

In many industry applications it is neither possible nor desirable to implement speed sensors for control of induction motors because inverters can satisfy the speed control requirements, and from the standpoints of cost, size, noise immunity and reliability of the drive. However, these open-loop controlled inverters have their shortcomings, such as slow dynamic response, poor speed regulation, and limited speed control range. So, the development of shaft sensorless adjustable speed drive has become an important research topic [5, 6]. There are two major concerns in the sensorless speed control of induction motor drive. One is the decoupling and linearizing control scheme, and another is the rotor speed estimation algorithm. Both are highly dependent on the motor parameters. Although many speed estimation algorithms and sensorless control schemes [7] have been developed during

K. B. Mohanty is with Electrical Engg. Dept., NIT Rourkela – 769008. (e-mail: kbm@nitr.ren.nic.in)

N. K. De and A. Routray are with Electrical Engg. Dept., IIT Kharagpur – 721302.

the past few years, a simple, effective, and low sensitivity sensorless control scheme is a worth pursuing goal.

In the present paper, input-output linearization and decoupling control of induction motor is presented in Section II. In Section III, sensorless speed control scheme is discussed. Results are discussed in Section IV.

II. LINEARIZATION AND DECOUPLING CONTROL OF INDUCTION MOTOR

Induction motor model in the arbitrary rotating d-q reference frame, with stator current and rotor flux components as variables is considered. For decoupling of torque and flux, the d-axis is to be completely aligned along the rotor flux axis. This leads to the mathematical constraint :

$$\Psi_{qr} = 0 \quad \text{and} \quad \dot{\Psi}_{qr} = 0 \quad (1)$$

Equation (1) is satisfied, and decoupling obtained, when

$$\omega_{sl} = \frac{R_r L_m}{L_r} \cdot \frac{i_{qs}}{\Psi_{dr}} \quad (2)$$

When (2) is satisfied, the dynamics of the motor is:

$$\dot{i}_{ds} = -a_1 i_{ds} + a_2 \Psi_{dr} + \omega_e i_{qs} + c v_{ds} \quad (3)$$

$$\dot{i}_{qs} = -\omega_e i_{ds} - a_1 i_{qs} - P a_3 \omega_r \Psi_{dr} + c v_{qs} \quad (4)$$

$$\dot{\Psi}_{dr} = -a_4 \Psi_{dr} + a_5 i_{ds} \quad (5)$$

$$T_e = K_t \Psi_{dr} i_{qs} \quad (6)$$

where, $c = L_r / (L_s L_r - L_m^2)$,

$$a_1 = c R_s + c R_r L_m^2 / L_r^2, \quad a_2 = c R_r L_m / L_r^2,$$

$$a_3 = c L_m / L_r, \quad a_4 = R_r / L_r,$$

$$a_5 = R_r L_m / L_r, \quad K_t = 3 P L_m / 2 L_r.$$

In the induction motor model described by (3-6), nonlinearity and interaction still exist. The transition from field oriented voltage components, v_{ds} and v_{qs} to current components as in (3) and (4), involves leakage time constants and interactions. As the developed torque is a product of Ψ_{dr} and i_{qs} , the overall system remains coupled. The interaction between current components, and nonlinearity in the overall system are eliminated by using input-output linearizing and decoupling control approach [1, 4, 8]. This approach consists of change of coordinates and use of nonlinear inputs to linearize the system equations. Developed torque, T_e is considered as a state variable, replacing i_{qs} to describe the motor dynamics. Then corresponding dynamic equation is:

$$\dot{T}_e = -(a_1 + a_4)T_e + K_t \Psi_{dr} [c v_{qs} - P \omega_r (i_{ds} + a_3 \Psi_{dr})] \quad (7)$$

Nonlinear control inputs of the form, u_1 and u_2 are used to linearize (3) and (7) as described in [8]. The input voltages, v_{ds} and v_{qs} to the motor in terms of u_1 and u_2 are:

$$v_{ds} = (-\omega_e i_{qs} + u_1) / c \quad (8)$$

$$v_{qs} = [P \omega_r (i_{ds} + a_3 \Psi_{dr}) + u_2 / K_t \Psi_{dr}] / c \quad (9)$$

III. SENSORLESS SPEED CONTROL

The block diagram of the linearized, decoupled, sensorless speed control scheme is shown in Fig. 1. This sensorless speed control system consists of three major parts: (A) Linearizing and Decoupling Controller, (B) Flux-weakening Controller, (C) Speed Estimator.

(A) Linearizing and Decoupling Controller

The linearizing and decoupling algorithm is described by (2), (8-9), and implemented through a software controller.

(B) Flux-weakening Controller

The flux weakening controller is used to regulate the magnitude of rotor flux linkage command Ψ_{dr}^* such that the motor will operate in constant torque mode when motor speed is below base speed and in constant power mode when motor speed is above the base speed. The flux weakening control algorithm is as follows.

$$\Psi_{dr}^* = \begin{cases} \Psi_R & \text{if } \hat{\omega}_r \leq \omega_b \\ \Psi_R \frac{\omega_b}{\hat{\omega}_r} & \text{if } \hat{\omega}_r \geq \omega_b \end{cases} \quad (10)$$

where, Ψ_R = rated rotor flux linkage in V·s

ω_b = base speed in rad/s

(C) Speed Estimator

In the speed estimation scheme described here, the synchronous speed is estimated and the slip speed is assumed to be command value required for decoupling control. So, the estimated rotor speed is given by:

$$\hat{\omega}_r = (\hat{\omega}_e - \omega_{sl}^*) / P \quad (11)$$

The principle of synchronous speed estimation is explained here. If $\Psi_{\alpha s}$ and $\Psi_{\beta s}$ are the two components of the stator flux vector in the stationary (α - β) reference frame, the electrical angle of the stator flux vector is defined as:

$$\theta_{\Psi_s} = \tan^{-1} (\Psi_{\beta s} / \Psi_{\alpha s}) \quad (12)$$

The time derivative of stator flux angle gives the instantaneous electrical synchronous speed.

$$\omega_e = \dot{\theta}_{\Psi_s} = \frac{\Psi_{\alpha s} \dot{\Psi}_{\beta s} - \Psi_{\beta s} \dot{\Psi}_{\alpha s}}{\Psi_{\alpha s}^2 + \Psi_{\beta s}^2} \quad (13)$$

From the voltage equations of the induction motor in the stationary (α - β) reference frame, the derivatives of the stator flux components are :

$$\begin{aligned} \dot{\Psi}_{\alpha s}(k) &= v_{\alpha s}(k) - R_s i_{\alpha s}(k) \\ \dot{\Psi}_{\beta s}(k) &= v_{\beta s}(k) - R_s i_{\beta s}(k) \end{aligned} \quad (14)$$

The stator flux components are then obtained as:

$$\begin{aligned} \Psi_{\alpha s}(k) &= \Psi_{\alpha s}(k-1) + \dot{\Psi}_{\alpha s}(k) T_s \\ \Psi_{\beta s}(k) &= \Psi_{\beta s}(k-1) + \dot{\Psi}_{\beta s}(k) T_s \end{aligned} \quad (15)$$

The command value of slip speed, ω_{sl}^* in (11) is the value required for decoupling control, and given by (16).

$$\omega_{sl}^*(k) = \frac{2}{3} \cdot \frac{R_r}{P} \cdot \frac{T_e^*(k)}{|\Psi_{dr}^*(k)|^2} \quad (16)$$

$T_e^*(k)$ = reference torque in N·m, generated from the speed error, through the speed controller.

In the calculation of the rotor angular speed, the sampling time is set at the same value (T_s) as used in the current control loop, to obtain a fast dynamic response. However, in this way the estimated speed is also corrupted by the current ripples. In practical conditions, the time constant of current loop is much smaller than that of the speed loop. In other words, the current loop bandwidth is much wider than the speed loop bandwidth. Therefore, a moving average algorithm [9] is used to smooth the estimated speed. The formula used is:

$$\hat{\omega}_r(n) = \frac{1}{N} \sum_{k=1}^N \hat{\omega}_r(n-k) \quad (17)$$

where, $N = T_2 / T_1$

T_1 = sampling time of the current control loop

T_2 = sampling time of the speed control loop

In the simulation study presented below, the values of T_1 and T_2 are 0.1 ms and 50ms, respectively.

IV. RESULTS AND DISCUSSIONS

The simulation study of the drive system has been carried out, with the rotor speed estimated, and the estimated speed used in the input-output linearizing and decoupling control algorithm. The rating and parameters of the induction motor used in the simulation study are given in Table I.

TABLE I

RATING AND PARAMETERS OF THE MOTOR

0.75 kW, 220V, 3A, 1440 rpm, 3-phase, 50 Hz.

$R_s = 6.37 \Omega$, $R_r = 4.3 \Omega$, $L_s = L_r = 0.26$ H,

$L_m = 0.24$ H, $J = 0.0088$ Kg·m², $\beta = 0.003$ N·m·s/rad.

The simulation result is presented in Fig. 2, for a step change in speed command from 1000 r/min to 1300 r/min. The command flux linkage is 0.45 V·s, i.e., the command d-axis stator current is 1.863 A. The speed response exhibits an overshoot of 109 r/min and 1% settling time of 0.3 s. The estimated speed response is similar to the actual speed response, except the fact that it contains ripple of peak-to-peak value, 50 r/min (1.36% rms) about the steady state value. The d-axis stator current exhibits overshoot of 0.252 A and oscillation for 0.18 s. The q-axis stator current exhibits overshoot of 5.7 A and oscillation for 0.45 s. Peak phase current of stator increases from 2 A to 6 A and exhibits oscillation for 0.14 s during the transient period.

For a step change in speed command from 1500 r/min to 1600 r/min with weakening of command flux linkage from 0.45 V·s to 0.422 V·s, the simulation result is presented in Fig. 3. Corresponding to this flux weakening, the command d-axis stator current is reduced from 1.863 A to 1.747 A. The speed response exhibits an overshoot of 65 r/min and 1% settling time of 0.32 s. The estimated speed response is similar to the actual speed response, except the fact that it contains ripple of peak-to-peak value, 70 r/min (1.547% rms) about the steady state value. The d-axis stator current exhibits undershoot of 0.05 A and oscillation for 0.3 s. The q-axis

stator current exhibits overshoot up to 2.55 A and oscillation for 0.72 s. It also contains peak-to-peak ripple of 0.44 A. Peak phase current of stator increases from 2 A to 3.15 A and exhibits oscillation for 0.3 s during the transient period.

V. CONCLUSIONS

The successful implementation of sensorless induction motor (IM) drive depends on not only fast and accurate rotor speed estimation, but also on well tuned decoupling control of the induction motor. The presented sensorless speed control scheme employs input-output linearization and decoupling control. A stator flux based flux estimator is used to estimate the speed. Studies show that, even if the estimated speed contains ripples, the actual speed response, with the controller using the estimated speed, is ripple free.

VI. REFERENCES

[1] D. I. Kim, I. J. Ha and M. S. Ko, "Control of induction motors via feedback linearization with input-output decoupling," *Int. Jou. of Control*, vol. 51, no. 4, 1990, pp. 863-883.
 [2] Z. Krzeminski, "Nonlinear control of induction motor," *IFAC 10th World Congress on Automatic Control*, vol. 3, Munich, 1987, pp. 349-354

[3] A. De Luca, and G. Ulivi, "Design of exact nonlinear controller for induction motors," *IEEE Trans. on Automatic Control*, vol. 34, no. 12, Dec. 1989, pp 1304-1307.
 [4] R. Marino, S. Peresada, and P. Valigi, "Adaptive input-output linearizing control of induction motors," *IEEE Trans. on Automatic Control*, vol. 38, no. 2, 1993, pp. 208-221.
 [5] K. Ohnishi, N. Matsui, and Y. Hori, "Estimation, identification and sensorless control in motion control system," *Proc. of IEEE*, vol.82, no.8, Aug. 1994, pp. 1253-1265.
 [6] J. Holtz, "Speed estimation and sensorless control of AC drives," *IEEE IECON Conf. Rec.*, vol. 2, 1993, pp. 649-654.
 [7] K. Rajashekara, A. Kawamura, and K. Matsuse, *Sensorless Control of AC Motor Drives*, Piscataway, NJ, IEEE Press, 1996.
 [8] K. B. Mohanty and N. K. De, "Nonlinear controller for induction motor drive," *Procc. of IEEE Int. Conf. on Industrial Technology (ICIT)*, 2000, Goa, India, pp. 382-387.
 [9] K. B. Mohanty, A. Routray, N. K. De, "Rotor flux oriented sensorless induction motor drive for low power applications", *Procc. of Int. Conf. - CERA*, Feb. 2002, India, pp. 747-752.

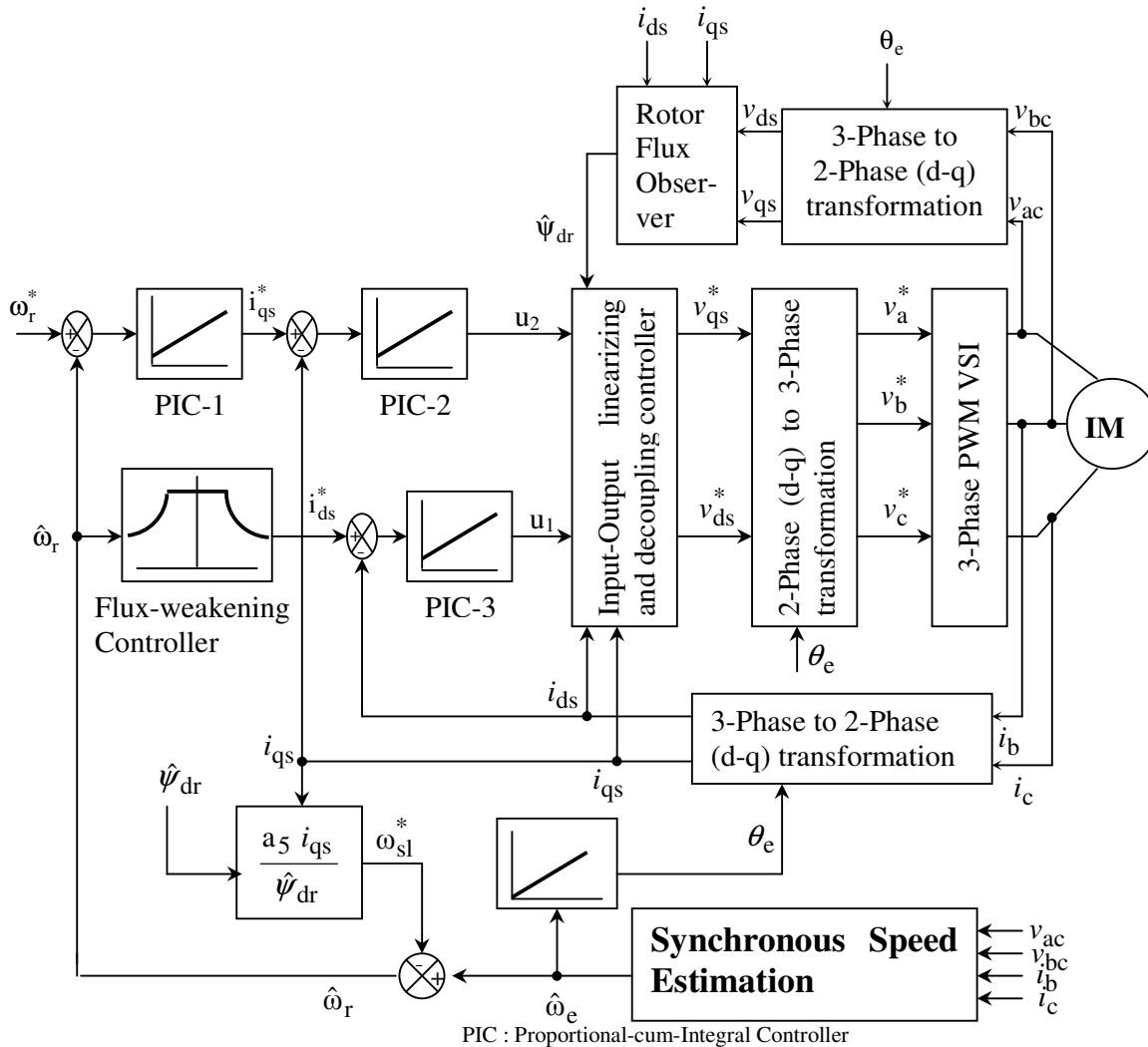


Fig. 1 Block diagram of the linearized, decoupled, sensorless speed control scheme

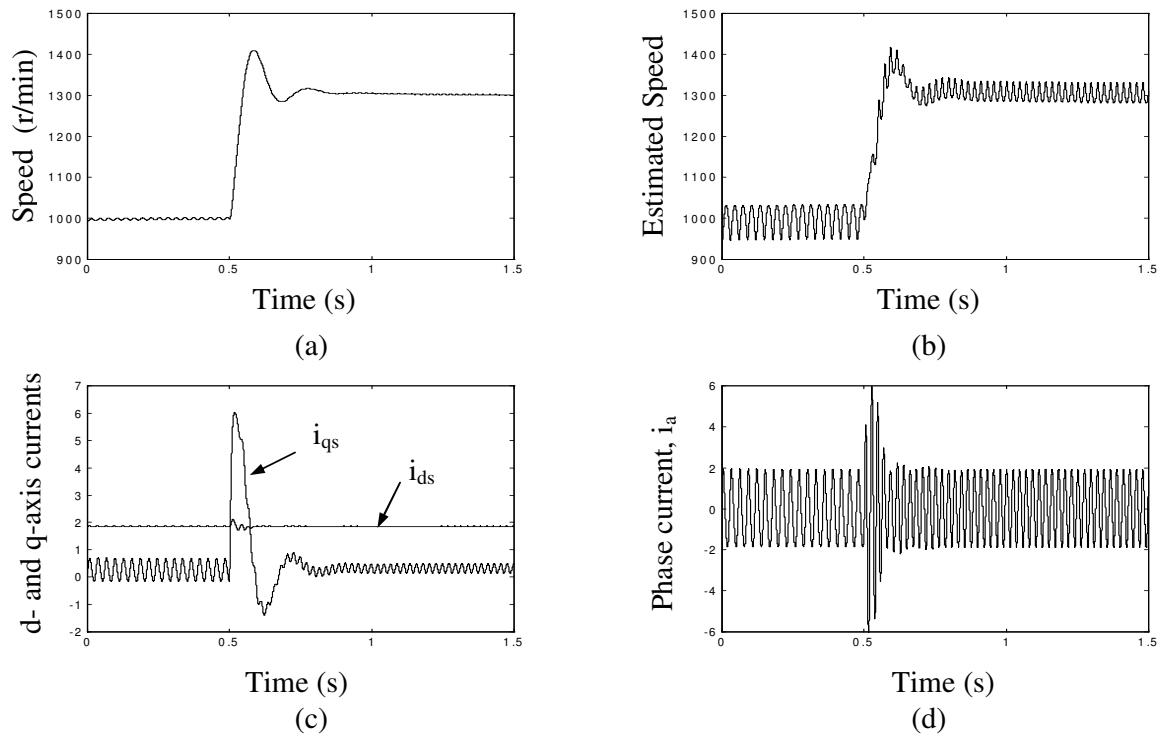


Fig. 2 Simulation responses for step change in speed with speed estimation: (a) Speed, (b) Estimated speed, (c) d- and q-axis stator currents, (d) Stator phase current,

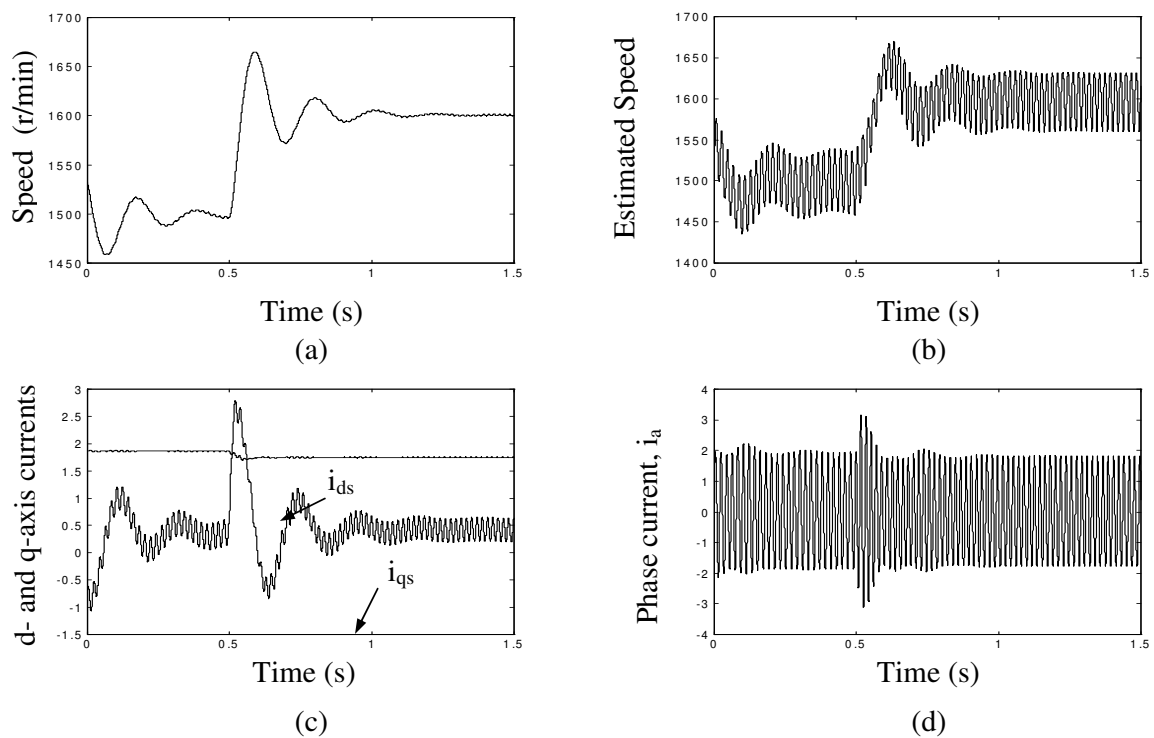


Fig. 3 Simulation responses for step change in speed with flux weakening and speed estimation: (a) Speed, (b) Estimated speed, (c) d- and q-axis stator currents, (d) Stator phase current